

Role of Metal(II) Hexacyanocobaltate(III) Surface Chemistry for Prebiotic Peptides Synthesis

Anand Kumar

SGRR (PG) College

Babita Saroha

UIET

Indra Bahadur (✉ bahadur.indra@nwu.ac.za)

North-West, South Africa

Devendra Singh Negi

H. N. B. Garhwal University

Monika Vats

ASAS, Amity University

Research Article

Keywords: Glycine, Alanine, Catalyst, MHCCo, Oligomerization, HPLC, ESI-MS

Posted Date: April 15th, 2022

DOI: <https://doi.org/10.21203/rs.3.rs-1507937/v1>

License: © ⓘ This work is licensed under a Creative Commons Attribution 4.0 International License. [Read Full License](#)

Abstract

Double metal cyanide (DMC), a heterogeneous catalyst, is a key factor for polymerization of amino acids. Based on the hypothesis, the present study is designed to evaluate favorable environmental conditions for the chemical evolution and origin of life such as effects of temperature and time for the oligomerization of glycine and alanine on Metal(II) Hexacyanocobaltate(III), MHCCo. It has been shown that MHCCo is porous and because of high surface area it has outstanding catalytic properties. Our results revealed that the Manganese(II) Hexacyanocobaltate(III) (MnHCCo), Iron(II) Hexacyanocobaltate(III) (FeHCCo), Nickel(II) Hexacyanocobaltate(III) (NiHCCo) complexes condense the glycine up to trimer and alanine up to dimer while ZnHCCo showed most valuable catalytic properties that changes glycine into tetramer and alanine into dimer with the high yield. High-Performance liquid chromatography (HPLC) and Electron Spray Ionizations-Mass spectroscopy (ESI-MS) techniques were used to confirm the oligomer products of glycine and alanine formed on MHCCo complexes. The results also exposed the catalytic role of MHCCo for the oligomerization of biomolecules thus supports the chemical evolution.

1. Introduction

Origin of life is still a mystery to the scientific world most prevalent question in science is how life emerges on earth. Earliest fossil evidences suggest life on earth prior 3.35Ga [1, 2] and according to molecular clocks origin was prior to 3.35 Ga [3]. Evolution might have not resulted from a sudden event it occurs due to series of events even the cell complexities have not appeared at once. Cooperative interactions between bio-polymers of different classes are a hallmark of biology [4]. In the ribosomes RNA makes protein and in polymerase protein makes RNA [5]. The contradiction between metabolism and genetics which comes first is still in play. The first paradigm advocates that there was an RNA world where dual roles were played by RNA as a catalyst and as a genetic polymer. With time the pure RNA gave rise to proteins and DNA on the course to the present biological system of RNA/DNA/Protein. The second paradigm supports that life originated from the protein prior to replicators' existence, where pseudo-replication of GADV (guanine, adenine, aspartic acid, valine) proteins occurs. Generation of peptides from amino acids with structure and function, a chemical evolution is a concern to origin of life research [6, 7]. It is still a matter of debate which come metabolism first or genetics first for the scientists till today whereas there are some research present which can attempt to solve this problem [8, 9]. Cooperative relationship among molecules also might have extended probable mechanism for the buildup and perseverance of certain molecules in the prebiotic environment. [7]. Navrotsky et al. 2021 suggested that amino acids, small peptides and fatty acids might acted as structure directing agents for functional porous silica structure gathering that promotes polymerization of amino acids and peptides along with other organic reactions [10]. Amino acids are the building block, as well as essential components for the formation and growth of life. Proteins act as catalyst in biochemical reactions, building materials for living cell, structural role inside the cell and found within the cell membrane. In the origin of life, formation of amino acids may have been an important route [11]. Since the pioneering experiments of Miller, it is extensively accepted that carbon, hydrogen, ammonia and water present in the early atmosphere, under the influence of electric discharge, are able to produced amino acids [12, 13]. The prebiotic soup would likely have been extremely dilute with respect to amino acid concentrations vary from $4 \times 10^{-3}M$ to $10^{-7}M$ [14–18]. Polymerization of biomonomers was the next step in the origin life, but the major problems mainly are low concentration and the short life times of amino acid in the many environments. As suggested by Bernal (1951) in prebiotic reactions which produce polymeric substances, life minerals has a pivotal role from which emergence of life takes place [19]. Biomonomers concentration and oligomerization by catalyst

might happen because of minerals during the chemical evolution. There are number of conditions which influence amino acid adsorption and binding by minerals/metal oxides/DMC as mentioned in previous studies [20–24].

Erastova et al. 2017 also indicated that minerals provide surface and thus afford peptide bond formation in prebiotic environment [25]. Amino acids and their condensation for the formation of peptide /proteins are vital in prebiotic chemistry as it is the key reaction for present life which involves amino acids/peptides/proteins [26].

Clay mineral as a heterogeneous catalyst for amino acid condensation has been widely accepted for primitive peptide bond formation [27–32]. Active surface and edges on the clay minerals (kaolinite and montmorillonite) formed the prebiotic peptide [33–36]. Reactivity on the adsorption process was quite slow, and condensation of few oligomers occurs still it play crucial role not only to concentrate the peptides but also stabilizing the peptide, disfavors the hydrolysis, leading to chain elongation propagation of formed peptides [36]. Pure silica and alumina have also been investigated in this context, showing even more favorable properties than composite natural minerals [37–43].

Metal ions play significant function in prebiotic chemistry, for the glycine and alanine polymerization [44]. Egami (1975) found that the concentration of minor transition elements (Mo, Zn, Fe, Cu, Mn, and Co) in primeval sea to be 7-100nM [45]. Later it was proposed that divalent transition metal ions might have formed complex compounds by using simple biomolecules which settled at the bottom of the sea shore. It may provide surface as a result interaction; oxidation and condensation process occurs and may help in the problem of polymerization of amino acid in aqueous solution [46].

In this paper, we evaluated the catalytic ability of MHCCo complexes for the formation of prebiotic peptides. Series of MHCCo complexes synthesis are described in the current work. In particular, we investigated polymerization of glycine and alanine without using drying/wetting cycle, as MHCCo complexes as catalyst. Entire experiment is carried out at different temperature 60 °C to 120 °C for the time of 5 weeks.

2. Materials And Methods

2.1. Chemicals required

Potassium hexacyanocobaltate (III) (Fluka), $Mn(NO_3)_2$ (E. Merck), $Fe(NO_3)_2$ (E. Merck), $Ni(NO_3)_2$ (E. Merck), $Zn(NO_3)_2$ (E. Merck). Sodium hexane sulphonate, H_3PO_4 , CH_3CN (HPLC grade) and standard of peptides were purchased from Sigma-Aldrich. During the experimental studies throughout Millipore water was used.

2.2. Preparation of Metal Hexacyanocobaltate (III)

Kaye and Long, 2005 method [47], followed for the synthesis of MHCCo complexes from potassium hexacyanocobaltate(III). 10 mmol of potassium hexacyanocobaltate(III) dissolved in 100 mL Millipore water, the solutions thus formed was added to the solution of 18 mmol metal nitrate in 100 mL Millipore water drop wise. The precipitate formed was allowed to anneal in the mother liquor and filtered on bucker funnel. The formed precipitate washed with Milli pore water, dried at 60 °C, powdered and sieved with 100 mesh size.

2.3. CHN, TGA/DTA, XRD

ElementarVario ELHI CHNS analyzer was used for carbon, hydrogen and nitrogen percentage present in MHCCo complexes analysis. Water of crystallization found in MHCCo complexes was monitored by Thermal

analyzer. 10°C/min heating rate was carried out throughout the measurement, while Al₂O₃ as a reference was used. X-ray diffraction technique was used for the authentication of MHCCo complexes. The relative-intensity data and interplanar spacing (d) were in good agreement with the reported values.

2.4. Infrared spectra

The vibration frequencies of synthesized MnHCCo, FeHCCo, NiHCCo and ZnHCCo complexes matched with the previously reported data [48–50]. The FT-IR spectra of MHCCo complexes were recorded in KBr pallet on a Perkin Elmer FTIR spectrophotometer.

2.5. Surface area measurement

The surface area of MHCCo complexes were analyzed by the Brunauer-Emmett-Teller (BET) [51] method on a surface area analyzer.

2.6. Reaction method

0.1 gram of MHCCo complexes and 0.1 mL of glycine and alanine amino acid (0.01M) were impregnated separately. For peptide bond formation examination, the suspension was dried at 90°C for 3h. Three different temperatures (60 °C, 90 °C, and 120 °C) was used for the analysis of peptide bond formation and was monitored for 5 weeks i.e 7, 14, 21, 28, 35 days. The sample was analyzed weekly. No fluctuating drying/wetting conditions were simulated. Glycine and alanine separately was used for the control experiment by heating at required temperature in an empty test tube of glass 150 x 15 mm. On completion of 1st week, adsorbed amino acids and related reaction products were released by treating peptides condensation products obtained with 1ml of 0.1M calcium chloride solution. The reaction product obtained was centrifuged and supernatant was analyzed by HPLC and ESI-MS analysis.

2.7 HPLC analysis

HPLC having column ((Spherisorp 5 µm ODS2 4.6mm × 250 mm) was used for the product analysis. The product was analyzed at 200 nm wavelength by UV detector. Sodium hexane sulphonate (10 mM) acidified with H₃PO₄ at a pH of ~ 2.5 (solvent A) and CH₃CN (solvent B) were used as mobile phase compositions at 1 ml/min flow rate. Identification of obtained products was done by retention times and later on co-injection method was used for further elucidation. Yield of the peptide bond formation was calculated by peak area of the products and standard comparison (indicated in supporting data S1-S4).

2.8 Electrospray Ionization–Mass Spectrometry analysis

ESI-MS spectral data were recorded on Bruker MicroTOF-Q II mass spectrometer on positive mode using direct injection method in the range m/z 50–500. The mass analysis of the product obtained was recorded by mass spectroscopy equipped with Electrospray ionization (ESI) source. Product ionization was done by following ESI setting: 10 psi Nebulizer gas flow, 300 °C temperature, 4000 V capillary voltage, 5 L min⁻¹ dry gas. In the presence of ZnHCCo complex, glycine and alanine were heated for 4 weeks at 90 °C, and the ESI MS spectra of the product analyzed.

2.9 Field Emission Scanning Electron Microscopy FE-SEM

The 2-D imaging, internal structure, and morphology of the complexes MnHCCo, FeHCCo, NiHCCo and ZnHCCo were analyzed with the help of FE-SEM.

2.10 Statistical Analysis:

All the experiments were performed in triplicates and the results recorded as mean of the triplicate measurements.

3. Results And Discussion

The first step of the material characterization is to identify the purity of the crystalline complexes. Figure 1a-d represents MnHCCo, FeHCCo, NiHCCo and ZnHCCo complexes XRD patterns. JCPDS diffraction files are used for analyzing the XRD pattern of MHCCo complexes. Diffraction peaks obtained are carefully matched with the relative intensities of the MHCCo complexes, JCPDS file no. for MnHCCo (22-1167), JCPDS file no. for FeHCCo (89-3736), JCPDS file no. for NiHCCo (22-1184) and JCPDS file no. for ZnHCCo (32-1468). The FT-IR spectrum of MHCCo complexes showed four significant peaks. In case of ZnHCCo, the band occurs at 2181 cm^{-1} corresponds to strong CN stretching frequency, at 1607 cm^{-1} peak represents the O-H bending of interstitial water molecules, 700 cm^{-1} occurs due to bending of metal-carbon while band occurs at 451 cm^{-1} represent the metal-cyanide bending. The bands occur due to other MHCCo complexes are indicated in Table 1.

The MHCCo complexes were further characterized by TG/DT analysis. Figure 2a-d represents the obtained thermograms. With the help of TG curve of MHCCo complexes, degree of hydration was calculated. Figure 2a represent thermogram for MnHCCo complexes that indicated mass loss which corresponds to nearly two water molecules, FeHCCo complex showed a mass loss of three water molecules (Fig. 2b), NiHCCo complex showed a mass loss of three water molecules (Fig. 2c), ZnHCCo complex showed a mass loss of four water molecules (Fig. 2d). The percentage of C, H, N in the MHCCo complexes were analyzed by CHNS analysis and are depicted in Table 2. The experimental results obtained by elemental analysis matched with the theoretical value. The synthesized MHCCo complexes were analyzed by XRD, CHN analysis, TG/DTA, are as follows:

1. $\text{Mn}_3[\text{Co}(\text{CN})_6]_2 \cdot 2\text{H}_2\text{O}$ (Brown) ;

2. $\text{Fe}_3[\text{Co}(\text{CN})_6]_2 \cdot 3\text{H}_2\text{O}$ (Blue);

3. $\text{Ni}_3[\text{Co}(\text{CN})_6]_2 \cdot 3\text{H}_2\text{O}$ (Sky Blue);

4. $\text{Zn}_3[\text{Co}(\text{CN})_6]_2 \cdot 4\text{H}_2\text{O}$ (White)

The Fig. 3a, 3b, 3c and 3d show the FE-SEM images and EDX spectra of MnHCCo, FeHCCo, NiHCCo and ZnHCCo respectively. The structural morphology of FeHCCo, NiHCCo and ZnHCCo particles was observed to be spherical and even, whereas that of MnHCCo particles appeared to be polygon in shape (square shape was observed mostly). The particles size of FeHCCo, NiHCCo and ZnHCCo was found to be uniform suggesting a narrow size distribution, and that of MnHCCo particles was found to be non-uniform suggesting a wide size distribution. The energy dispersive X-ray (EDX) spectra clearly indicate the presence of the corresponding metal in the MHCCo complexes.

To find the catalyzing properties of the MHCCo complexes, the oligomerization reaction of amino acid (glycine and alanine) were carried out at varies temperature i.e 60, 90, 120°C for 5 weeks (7, 14, 21, 28, 35 days) in the

presence of MHCCo complexes. We studied the effects of temperature and time for the glycine and alanine oligomerization on MHCCo complexes. The catalytic efficiency of tested MHCCo complexes varies considerably with time and temperature are shown in Fig. 4(a-c) to 7(a-c). The yields of MHCCocatalyzed glycine and alanine oligomerization at different temperature 60, 90, 120°C on a completion of 5th week are summarized in Table 3 and Table 4. It is found that, product yield Vs time as functions of temperature behave linear relationship. The yields on MHCCo complexes are much higher than those produced in blank experiment. On the completion of 5th week, diketopiperazine (DKG) of glycine and dimer of glycine, Glycyl-glycine (gly)₂ was found in experiments of glycine without catalyst, while peptide formation was not obtained in experiment of alanine without catalyst. Formation of DKG (glycine), dimer of glycine and absence of condensation of alanine in the control experiment from glycine and alanine in absence of MHCCo complexes, the results is in accord with the previous studies [39, 52]. MHCCo complexes provide the surface for catalyzing the thermal condensation of glycine and alanine at relatively short time at temperature below 100°C. For identification and quantification of the obtained product in the reaction mixtures were analyzed by HPLC and ESI-MS techniques. The analysis of the reaction products by HPLC and ESI-MS revealed that peptides up to tetramer were formed from glycine while dimer in case of alanine. The Fig. 8(a-d) and 9(a-d) represent the HPLC chromatogram showing the separation of diketopiperazine, oligomers of glycine and alanine at optimum conditions. In the experiment, reaction was performed at varied temperature from 60 to 120°C for 5 weeks without applying dry/ wetting cycle. The reaction was monitored per week.

When we compared the runs, on the completion of 5th week, at lower temperature i.e. 60°C, only trimer of glycine, Glycyl-glycyl-glycine (Gly)₃ were observed in the presence of Mn-, Zn-HCCo and dimer of alanine (Ala)₂ were observed in the presence of all three MHCCo complexes except FeHCCo but with low yield (Fig. 4a-7a) and without the presence of localized heat sources. Thus, in the presence of MHCCo, abiotic peptide synthesis occurs at short interval of time. It was observed that when the reaction temperature was 90°C, peptide was formed after short reaction times i.e. after 1 week in both the glycine and alanine with comparable yield. It has been found that yield of peptides were maximum on the completion of 4th week (Fig. 4b-7b) and after that it was constant even at high temperature (Fig. 4c-7c). Thus our result reveals that the favorable condition for the polymerization of amino acids on the surface of MHCCo complexes are 90°C temperature and duration is 4 weeks. But in case of formation of DKP (Gly) and DKP (Ala) on MHCCo complexes, it was observed that formation was more favorable from thermodynamic and kinetic point of view. DKP (Gly) and DKP (Ala) showed high yields, may be due to the low concentration of aqua layer on the MHCCo surface as compared to surrounding temperature at 120°C which do not favor elongation instead supports removal of water molecules from the dimeric glycine and alanine. In this study we found that high temperature supports the formation of DKPs, previously reported studies also revealed the same results [24, 31, 40]. Under hydrothermal conditions, rate of reaction for the formation of dimer and DKPs was also studied by Kawamura and co-workers [53, 54]. Bujdak and Rojas [55] found that polymerization of glycine and alanine using three different form of alumina i.e., acidic, neutral and basic and observed when neutral alumina used as a catalyst shows maximum polymerization of glycine and alanine. Activated alumina has been used as energy source for peptide bond formation [40], and this activated alumina oligomerize glycine upto (gly)₁₁ [56]. Catalytic activity of Ferrihydrite is due to its nanoporous high surface which dimerize glycine and alanine [57]. According to Ferris, oligomer upto 55 monomer long have been formed by using mineral surface [58] while glycine condensation upto 16 unit (poly-Gly) have been done on SiO₂ and TiO₂ surface [59]. At low temperature (-20°C) by using carbon dots as a photocatalyst polymerize amino acids to protein [60]. Glycine polymerization by thermal condensation occurs on SiO₂ [61] and metal ferrite surface [62].

Double metal cyanide (DMC), $M_a^I[M^{II}(CN)_n]_b \cdot xH_2O$ is an inorganic coordinated complexes with 3D network. In DMC, inner metal M^{II} is allied with the external metal M^I by number of cyano-bridges ($M^{II}-C \equiv N-M^I$) where M^I =divalent metal ions (Zn^{2+} , Fe^{2+} , Cd^{2+} , Co^{2+} , Cu^{2+} , Ni^{2+} , Mn^{2+} etc.) and M^{II} =transitional metal ions (Fe^{2+} , Fe^{3+} , Co^{2+} , Ni^{2+} , Cr^{3+} , Mo^{4+} etc.). In DMC, the active site is the external metal M^I which supports the catalytic functions. It was examined that DMC having varies inner and outer spheremetalsexhibited different catalytic properties. If external metal is zinc on the surface of octacyanomolybdate (IV), exhibited higher catalytic activity for the formation of oligomers of glycine and alanine, compared with octacyanomolybdate (IV) having other metals such as Mn^{2+} , Fe^{2+} , Co^{2+} , Ni^{2+} , Cu^{2+} , Cd^{2+} [24]. Present results showed that hexacyanocobaltate complexes having zinc as an external metal also showed evidence of high catalytic activity towards glycine and alanine i.e formation of oligomers of glycine and alanine, compared to other metals in outer sphere of hexacyanocobaltate complexes such as Mn^{2+} , Fe^{2+} , Ni^{2+} . The Table 3 and Table 4 shows the % yield of Cyclic (Gly)₂, di-, tri-, tetramer of glycine and Cyclic(Ala)₂, dimer of alanine on the surface of MHCCo complexes. It was also observed that ZnHCCo and MnHCCo oligomerize glycine upto tetramer, NiHCCo afforded glycine upto the trimer while the FeHCCo oligomerize upto the dimer. ZnHCCo complex formed (Gly)₄ (0.36%), (Gly)₃ (1.19%), (Gly)₂ (11.97%), DKP(Gly) (15.73%) from glycine while (Ala)₂ (6.27%), Cyclic(Ala)₂ (8.31%) formed from alanine on the completion of 5th week (35 days) at 90°C temperature. From the present study we also revealed that yield of glycine oligomers in the presence of MHCCo complexes is much more than that of oligomer of alanine, due to high activation energy required for alanine oligomerization [63]. Lower amount and efficiency of catalytic sites may be the other factor which can be responsible for lower oligomerization of alanine on MHCCo complexes [64]. Greenstein reported that stability constants of co-ordination complexes with amino acids are higher than the peptides supports the formation of oligomers of glycine and alanine [65]. This mechanism revealed that as the chain length of amino acid elongates, oligomers concentration decreases (Table 3 and Table 4). On the basis of % yield of glycine and alanine oligomers in the presence of MHCCo complexes shows following catalytic activity trend:

ZnHCCo > MnHCCo > NiHCCo > FeHCCo

Surface area of MHCCo complexes (Table 5) and the yield of peptide bond formation (Table 3 and Table 4), observed that surface area of MHCCo complexes plays an important parameter for the polymerization of amino acids. Among MHCCo, ZnHCCo has highest surface area ($683 \text{ m}^2\text{g}^{-1}$) showed high catalytic activity for the peptide bond formation while FeHCCo has lower surface area ($S.A = 167 \text{ m}^2\text{g}^{-1}$) exhibited minimum catalytic activity.

The ESI-MS technique provide the additional analytical technique for the detection of oligomers of glycine and alanine in terms of mass, $m/z = (M + H)^+$ ions, M indicated the amino acid/oligomers to be analyzed. Figures 10 and 11 represents the ESI-MS spectrum of formation of oligomers of glycine and alanine respectively on the surface of ZnHCCo at optimum temperature on the completion of 4th week. The ESI-MS (Fig. 10) clearly supports the formation of DKP (glycine), dimer, trimer, tetramer of glycine. The 76.1 mass of glycine obtained in ESI-MS represents $[Gly + H]^+$, 115 for $[CycGly_2 + H]^+$, 132.9 for $[Gly_2 + H]^+$, 189.9 for $[Gly_3 + H]^+$, 246.6 for $[Gly_4 + H]^+$. Similarly in Fig. 11 ESI-MS for formation of oligomers of alanine such as DKP (alanine), dimer of alanine at optimum temperature on the completion of 4th week at the surface of ZnHCCo are shown. The 90.1 mass of alanine observed in ESI-MS represents $[Ala + H]^+$, mass value 143 and 160.9 corresponds to $[CycAla_2 + H]^+$ and

[Ala₂ + H]⁺ respectively. The both ESI-MS and HPLC data matched with results obtained throughout the experiments.

Divalent transition metal hexacyanocobaltates(III), in which central metal atom and carbon of cyanide group bonded through coordinate bond. It is found that these porous, water insoluble, mixed valency octahedral coordinated complexes are a part of Fm3m and Pm3m space group [47, 66] with reduced size and high surface area promoted high catalytic activity [47, 66–70]. In the present study, MHCCo complexes also showed high catalytic activity for the production of peptide bond formations because of mixed valency and high surface area. The evidences summarized above suggest catalytic activity of MHCCo complexes for the condensation of amino acids and thus supported the chemical evolution of life.

4. Conclusion

The present results support the possibility of role of MHCCo surface chemistry in origin of life. The consequence of time duration and temperature for the peptide bond formation on the surface of MHCCo complexes were studied. This is the first time that MHCCo has been investigated in the oligomerization of glycine and alanine without applying drying/wetting cycling. ZnHCCo was the most effective among MHCCo and form considerable amount of up to (0.36%) (Gly)₄ along with (1.19%) (Gly)₃, (11.97%) (Gly)₂ and (15.75%) Cyclic (Gly)₂ while in case of alanine (6.27%) (Ala)₂ and (8.31%) Cyclic (Ala)₂. High surface area may be the main parameter, which provides more area for chain elongation of glycine and alanine thus high yield of oligomers of amino acids on the surface of ZnHCCo. It may be proposed that the MHCCo present on the primordial ocean provide favorable conditions for production of prebiotic peptide bond, thus support the process of abiogenesis.

Declarations

Acknowledgments

Author (Dr. Anand Kumar) is thankful to the Ministry of Human Resource and Development (MHRD), New Delhi for providing financial assistance. Authors are also thankful to Prof Tokeer Ahmad, Department of Chemistry, Jamia Millia Islamia, New Delhi, for surface area analysis of the samples.

Author Contributions

Anand Kumar and Babita Saroha performed the research, analysed the data and wrote the first draft of the paper. Monika Vats analysed the data and substantially edited the first draft. Indra Bahadur and Devendra Singh Negi contributed methods to the paper and analysed the results as well as conceived the study and edited the final draft.

Conflict of interest

None to declare.

References

1. E.J. Javau, Challenges in evidencing the earliest traces of life, Nat. 572 (2019) 451–460.

2. A. Rimola, M. Sodupe, P. Ugliengo, Role of Mineral Surfaces in Prebiotic Chemical Evolution. In *Silico Quantum Mechanical Studies*, *Life* 9 (2019) 10–53.
3. H.C. Betts, M.N. Puttick, J.W. Clark, T.A. Williams, P.C.J. Donoghue, D. Pisani, Integrated genomic and fossil evidence illuminates life's early evolution and eukaryote origin, *Nat. Ecol. Evol.* 2 (2018) 1556–1562.
4. M. Frenkel-Pinter, J.W. Haynes, A.M. Mohyeldin, C. Martin, A.B. Sargon, A.S. Petrov, R. Krishnamurthy, N.V. Hud, L.D. Williams, L.J. Leman, Mutually stabilizing interaction between proto-peptide and RNA, *Nat. Comm.* 11 (2020) 3137-3151.
5. K.A. Lanier, A.S. Petrov, L.D. Williams, The central symbiosis of molecular biology: Molecules in mutualism, *J. Mol. Evol.* 85 (2017) 8–13.
6. G. Danger, R. Plasson, R. Parcal, Pathways for the formation and evolution of peptides in prebiotic environments, *Chem. Soc. Rev.* 41 (2012) 5416–5429.
7. M. Frenkel-Pinter, M. Samanta, G. Ashkenasy, L.J. Leman, Prebiotic peptides: Molecular hubs in the origin of life, *Chem. Rev.* 120 (2020) 4707–4765.
8. K. Kawamura, Hypothesis: Life Initiated from Two Genes, as Deduced from the RNA World Hypothesis and the Characteristics of Life-Like Systems, *Life* 6 (2016) 29–48.
9. K. Kawamura, Drawbacks of the ancient RNA-based life-like system under primitive earth conditions, *Biochimie.* 94 (2012) 1441–1450.
10. A. Navrotsky, R. Herviga, J. Lyonsa, D. Seo, E. Shocka, A. Voskanyana, Cooperative formation of porous silica and peptides on the prebiotic Earth, *PNAS.* 118 (2021).
11. A.I. Oparin, *The Origin of Life*, Moscow 1936.
12. S.L. Miller, A production of amino acids under possible primitive earth conditions, *Sci.* 117 (1953) 528–529.
13. S.L. Miller, Production of some organic compounds under possible primitive Earth conditions, *J. Am. Chem. Soc.* 77 (1955) 2351–2361.
14. A.D. Aubrey, H.J. Cleaves, J.L. Bada, Organic synthesis in submarine hydrothermal vent systems: I. Amino acids, *Orig. Life Evol. Biosph.* 39 (2009) 91–108.
15. H.J. Cleaves, A.D. Aubrey, J.L. Bada, An evaluation of the critical parameters for abiotic peptide synthesis in submarine hydrothermal systems, *Orig. Life Evol. Biosph.* 39 (2009) 109–126.
16. S.L. Miller, L.E. Orgel, *The Origins of Life on the Earth.* (1974) Prentice Hall, Englewood Cliffs, NJ.
17. R. Stribling, S.L. Miller, Energy yields for hydrogen cyanide and formaldehyde syntheses: the HCN and amino acid concentrations in the primitive ocean. *Orig. Life Evol. Biosph.* 17 (1987) 261–273.
18. N. Lahav, S. Chang, The possible role of solid surface area in condensation reactions during chemical evolution: reevaluation, *J. Mol. Evol.* 8 (1976) 357–380.
19. Bernal JD (1951) *The Physical Basis of Life*, Rourledge and Kegan Paul, London.
20. J. Goscianska, A. Olejnik, R. Pietrzak, Adsorption of L-phenylalanine onto mesoporous silica, *Mater. Chem. Phys.* 142 (2013) 586–593.
21. Q. Gao, Y. Xu, D. Wu, Y. Sun, Adsorption of amino acids on SBA-15-type mesoporous materials. *Stud. Surf. Sci. Catal.* 170 (2007) 961–966.
22. J.F. Lambert, Adsorption and polymerization of amino acids on minerals surface, *Orig. Life. Evol. Biosph.* 38 (2008) 211–242.

23. B.B. Tewari, N. Hamid, Interaction of glycine and beta alanine with nickel and cobalt and cadmium ferrocyanides, *Colloids and surface A: Physiochem. Eng. Aspects.* 296 (2007) 264–269.
24. A. Kumar, Kamaluddin, Oligomerization of glycine and alanine on metal(II) octacyano molybdate(IV): role of double metal cyanides in prebiotic chemistry, *Amino Acids*, 43 (2012) 2417–2429.
25. V. Erastova, M.T. Degiacomi, D.G. Fraser, H.C. Greenwell, Mineral surface chemistry control for origin of prebiotic peptides, *Nat. Commun.* 8 (2017) 2033–2042.
26. J. Darnell, H. Lodish, D. Baltimore, *Molecular cell biology* (1990). Scientific American Books, New York, p 48.
27. W. Martin, J. Baross, D.M. Kelley, C. Russell, Hydrothermal vents and the origin of life. *Nat. Rev. Microbiol.* 6 (2008) 805–814.
28. E.T. Degens, J. Matheja, T.A. Jackson, Template catalysis: Asymmetric polymerization of amino-acids on clay minerals, *Nat.* 227 (1970) 492–493.
29. T.L. Porter, M.P. Eastman, E. Bain, S. Begay, Analysis of peptides synthesized in the presence of SAz-1 montmorillonite and Cu²⁺ exchanged hectorite, *Biophys. Chem.* 91 (2001) 115–124.
30. A. Rimola, M. Sodupe, P. Ugliengo, Aluminosilicate surfaces as promoters for peptide bond formation: An assessment of Bernal's hypothesis by AB Initio methods. *J. Am. Chem. Soc.* 129 (2007) 8333–8344.
31. J. Wu, Z. Zhang, X. Yu, H. Pan, W. Jiang, X. Xu, R. Tang, Mechanism of promoted dipeptide formation on hydroxyapatite crystal surfaces, *Chin. Sci. Bull.* 56 (2011) 633–639.
32. C. Zuo, B.C. Zhang, B.J. Yan, J.-S. Zheng, One-pot multi-segment condensation strategies for chemical protein synthesis, *Org. Biomol. Chem.* 17 (2019) 727–744.
33. N. Lahav, D. White, S. Chang, Peptide formation in the prebiotic era: thermal condensation of glycine in fluctuating clay environments, *Sci.* 201 (1978) 67–69.
34. J.J. Flores, W.A. Bonner, On the asymmetric polymerization of aspartic acid enantiomers by kaolin. *J. Mol. Evol.* 3 (1974) 49–56.
35. J. Bujdak, H. Slosiarikova, N. Texler, M. Schwendinger, B.M. Rode, On the possible role of montmorillonites in prebiotic peptide formation, *Monatshefte. Fur. Chemie.* 125 (1994) 1033–1039.
36. J. Bujdak, K. Faybikova, A. Eder, Y. Yongyai, B.M. Rode, Peptide chain elongation: A possible role of montmorillonite in prebiotic synthesis of protein precursors, *Orig. Life Evol. Biosph.* 25 (1995) 431–441.
37. V.A. Basiuk, T.Y. Gromovoy, V.G. Golovaty, A.M. Glukhoy, Mechanisms of amino acid polycondensation on silica and alumina surfaces *Orig. Life Evol. Biosph.* 20 (1990) 483–498.
38. J. Bujdak, B.M. Rode, Silica, alumina, and clay-catalyzed alanine peptide bond formation, *J. Mol. Evol.* 45 (1997) 457–466.
39. J. Bujdak, B.M. Rode, Silica, alumina and clay catalyzed peptide bond formation: enhanced efficiency of alumina catalyst, *Orig. Life Evol. Biosph.* 29 (1999) 451–461.
40. J. Bujdak, B.M. Rode, Activated alumina as an energy-source for peptide-bond formation - consequences for mineral-mediated prebiotic processes, *Amino Acids.* 21 (2001) 281–291.
41. J. Bujdak, B.M. Rode, Alumina catalyzed reactions of Amino Acids, *J. Therm. Anal. Calorim.* 73 (2003) 797–805.
42. R. Saladino, G. Botta, B.M. Bizzarri, E.D. Mauro, J.M.G. Ruiz, A global scale scenario for prebiotic chemistry: Silica-based self-assembled mineral structures and formamide, *Biochem.* 55 (2016), 2806–2811.

43. M. Brodrecht, B. Kumari, A.S.S.L. Thankamony, H. Breitzke, T. Gutmann, G. Buntkowsky, Structural insights into peptides bound to the surface of silica nanopores, *Chem.* 25 (2019).5214–5221.
44. H. Paecht-Horowitz, The mechanism of clay catalyzed polymerization of amino acid adenylates, *Biosyst.* 9 (1977) 93–98.
45. F. Egami, Origin and early evolution of transition element enzymes, *J. Biochem.* 77 (1975) 1165–1169.
46. K. Kobayashi, C. Ponnampereuma, Trace elements in chemical evolution, I, *Orig. Life.* 16 (1985) 41–55
47. S.S. Kaye, J.R. Long, Hydrogen storage in the dehydrated Prussian blue analogues. *J. Am. Chem. Soc.* 127 (2005) 6506–6507.
48. C.P. Krap, B. Zamora, L. Reguera, E. Reguera, Stabilization of cubic and rhombohedral phases of zinc hexacyanocobaltate(III), *Microporous Mesoporous Mater.* 120 (2009) 414–420.
49. D.F. Mullica, J.D. Oliver, W.O. Milligan, F.W. Hills, Ferrous hexacyanocobaltate dodecahydrate. *Inorg. Nucl. Chem. Lett.* 15 (1979) 361–365.
50. D.F. Mullica, J.T. Zielke, E.L. Sappenfield, Synthesis, peripheral studies, and structural investigation of (1:1) $Mn_3[(Co/Cr)(CN)_6]_2 \cdot 14H_2O$, *J. Solid State Chem.* 112 (1994) 92–95.
51. S. Brunauer, P.H. Emmett, E. Teller, Adsorption of gases in multimolecular layers. *J. Am. Chem. Soc.* 60 (1938) 309–319.
52. J. Bujdak, B.M. Rode, The effect of clay structure on peptide bond formation catalysis. *J. Mol. Catal. A.* 144 (1999) 129–136.
53. K. Kawamura, T. Nishi, T. Sakiyama, Consecutive elongation of alanine oligopeptides at the second time range under hydrothermal conditions using a microflow reactor system, *J. Am. Chem. Soc.* 2005 (127) 522–523.
54. K. Kawamura, M. Yukioka, Kinetics of the racemization of amino acids at 225–275 C using a real-time monitoring method of hydrothermal reactions, *Thermo. Chimica. Acta* 375 (2001) 9–16.
55. V.A. Bujdak, J.S. Rojas, Catalysis of peptide formation by inorganic oxides: high efficiency of alumina under mild conditions on the earth-like planets. *Ad. Space Res.* 27 (2001) 225–230.
56. J. Bujdak, B.M. Rode, Peptide bond formation on the surface of activated alumina: peptide chain elongation, *Catal. Lett.* 91 (2003) 149–154.
57. G. Matrajt, D. Blanot, Properties of synthetic ferrihydrite as an amino acid adsorbent and a promoter of peptide bond formation, *Amino Acids* 26 (2004) 153–158.
58. J.P. Ferris, A.R. Hill, R. Liu, L.E. Orgel, Synthesis of Long Prebiotic Oligomers on Mineral Surfaces, *Nat.* 381 (1996) 59–61.
59. G. Martra, C. Deiana, Y. Sakhno, I. Barberis, M. Fabbiani, M. Pazzi, M. Vincenti, The formation and self-assembly of long prebiotic oligomers produced by the condensation of unactivated amino acids on oxide surfaces, *Angew. Chem. Int. Ed. Engl.* 53 (2014) 4671–4674.
60. H. Huang, S. Yang, Y. Liu, Y. Yang, H. Li, J.A. McLeod, G. Ding, J. Huang, Z. Kanga, Photocatalytic polymerization from amino acid to protein by carbon dots at room temperature, *ACS Appl. Bio Mater.* 11 (2019) 5144–5153.
61. M. Meng, L. Stievano, J. Lambert, Adsorption and thermal condensation mechanisms of amino acids on oxide supports. 1. Glycine on Silica, *Langmuir* 20 (2004) 914–923.

62. M.A. Iqbal, R. Sharma, S. Jheeta, Kamaluddin, Thermal Condensation of Glycine and Alanine on Metal Ferrite Surface: Primitive Peptide Bond, *Life* 7 (2017) 15–35.
63. J.G. Lawless, N. Levi, The role of metal ions in chemical evolution: polymerization of alanine and glycine in a cation-exchanged clay environment, *J. Mol. Evol.* 13 (1979) 281–286.
64. M.G. Schwendinger, B.M. Rode, Salt-induced formation of mixed peptides under possible prebiotic conditions, *Inorg. Chim. Acta* 186 (1991) 247–251.
65. J.P. Greenstein, M. Winitz, *Chemistry of amino acids*. (1961) New York: Wiley
66. M.R. Hartman, V.K. Peterson, Y. Liu, S.S. Kaye, J.R. Long, Neutron diffraction and neutron vibrational spectroscopy studies of hydrogen adsorption in the Prussian blue analogue $\text{Cu}_3[\text{Co}(\text{CN})_6]_2$, *Chem. Mater.* 18 (2006) 3221–3224.
67. L. Guadagnini, D. Tonelli, M. Giorgetti, Improved performances of electrodes based on Cu^{2+} loaded copper hexacyanoferrate for hydrogen peroxide detection. *Electro. Chim. Acta* 55 (2010) 5036–5039.
68. O.N. Risset, E.S. Knowles, S.Q. Ma, M.W. Meisel, D.R. Talham, Effects of lattice misfit on the growth of coordination polymer heterostructures, *Chem. Mater.* 25 (2013) 42–47.
69. A. García-Ortiz, A. Grirrane, E.R. Edilso, H. García, Mixed (Fe^{2+} and Cu^{2+}) double metal hexacyanocobaltates as solid catalyst for the aerobic oxidation of oximes to carbonyl compounds, *J. Catal.* 311 (2014) 386–392.
70. K. Zhang, R.S. Varma, H.W. Jang, J.-W. Choi, M. Shokouhimehr, Iron hexacyanocobaltate metal-organic framework: highly reversible and stationary electrode material with rich borders for lithium-ion batteries, *J. Alloys. Compd.* 791 (2019) 911–917.

Tables

Table 1
Infrared Spectral Frequencies (cm^{-1}) of
MHCCo complexes.

MHCCo	ν_{CN}	δ_{OH}	$\delta_{\text{M-C}}$	$\delta_{\text{M-CN}}$
MnHCCo	2170	1610	707	445
FeHCCo	2169	1607	695	456
NiHCCo	2175	1610	699	461
ZnHCCo	2181	1607	700	451

Table 2. CHNS analysis of MHCCo.

	C(%)	N(%)	H(%)
MnHCCo	21.51 (22.86)	25.61 (26.64)	0.53 (0.63)
FeHCCo	20.28 (22.12)	23.22 (25.79)	0.69 (0.92)
NiHCCo	20.99 (21.83)	24.98 (25.46)	0.85 (0.91)
ZnHCCo	22.07 (20.64)	24.94 (24.07)	1.27 (1.15)

* Bracket values are theoretical ones.

Table 3
Percent yield (%) of obtained products from glycine

Catalyst	Percent yield of obtained products from glycine at different temperature on the completion of 5th week											
	Cyc(Gly) ₂			(Gly) ₂			(Gly) ₃			(Gly) ₄		
	60 ⁰	90 ⁰	120 ⁰	60 ⁰	90 ⁰	120 ⁰	60 ⁰	90 ⁰	120 ⁰	60 ⁰	90 ⁰	120 ⁰
No Catalyst	0.04	0.06	0.10	Trace	0.02	0.03	-	-	-	-	-	-
MnHCCo	17.11	20.55	20.58	4.79	9.73	9.92	0.12	0.81	0.76	-	0.32	0.35
FeHCCo	3.31	40.50	44.11	0.10	0.20	0.22	-	-	-	-	-	-
NiHCCo	3.64	22.08	30.29	0.59	4.26	4.94	-	0.47	0.58	-	-	-
ZnHCCo	13.01	15.73	18.85	5.81	11.97	11.87	0.14	1.19	1.09	-	0.36	0.34

Table 4
Percent yield (%) of obtained products from alanine

Catalyst	Percent yield of obtained products from alanine at different temperature on the completion of 5th week					
	Cyc(Ala) ₂			(Ala) ₂		
	60 ⁰	90 ⁰	120 ⁰	60 ⁰	90 ⁰	120 ⁰
No Catalyst	0.02	0.04	0.06	-	-	-
MnHCCo	1.94	7.90	7.93	0.71	4.96	4.91
FeHCCo	1.70	22.76	22.47	-	-	-
NiHCCo	0.95	12.78	19.96	0.10	1.22	1.32
ZnHCCo	1.83	8.31	8.91	0.82	6.27	5.98

Table 5
Surface area of MHCCo complexes

MHCCo complexes	Surface area (m ² /g)
Mn ₃ [Co(CN) ₆] ₂ .2H ₂ O	615.26
Fe ₃ [Co(CN) ₆] ₂ .3H ₂ O	167.91
Ni ₃ [Co(CN) ₆] ₂ .3H ₂ O	572.39
Zn ₃ [Co(CN) ₆] ₂ .4H ₂ O	683.17

Figures

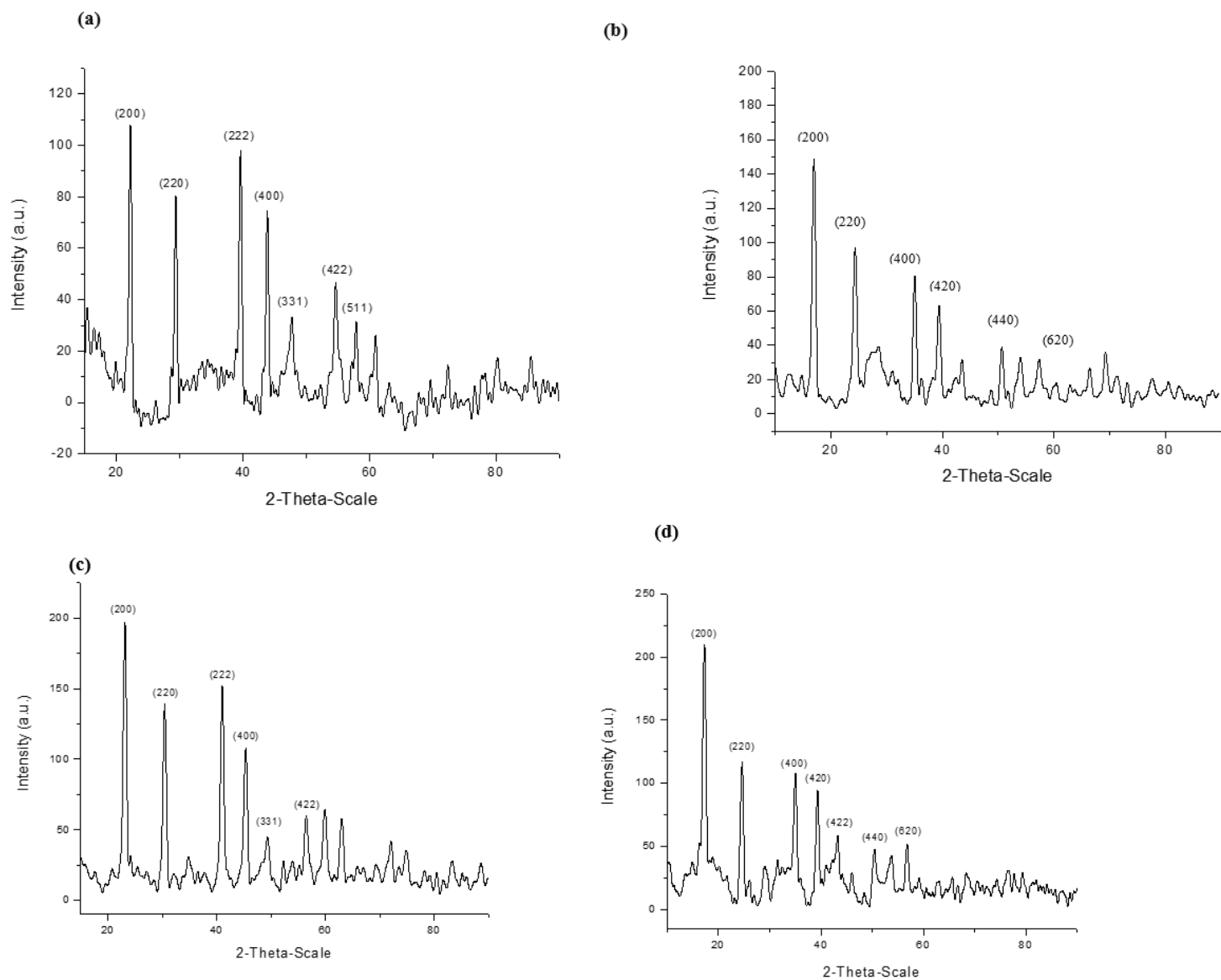


Figure 1

XRD data of (a) MnHCCo, (b) FeHCCo, (c) NiHCCo, (d) ZnHCCo.

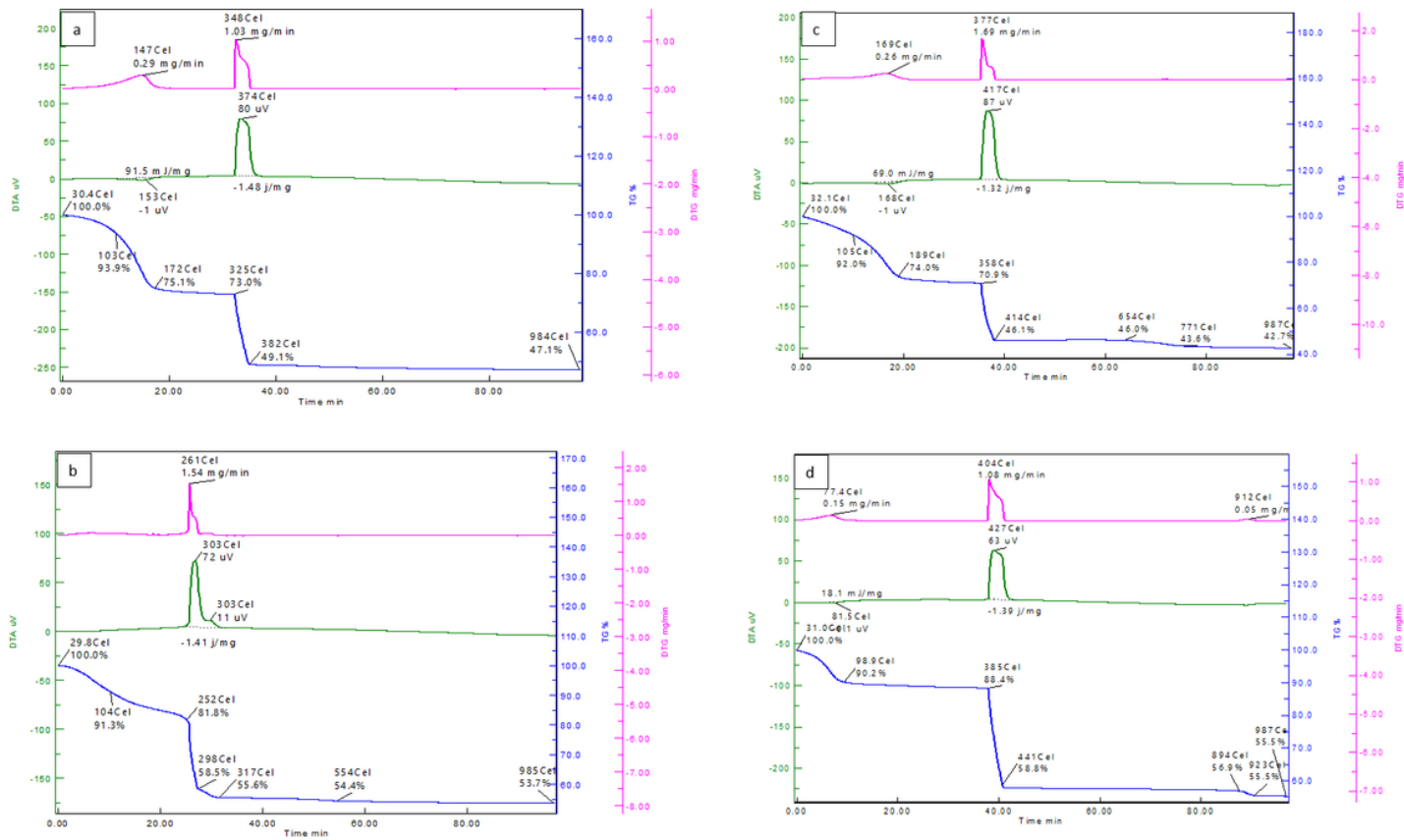


Figure 2

TG/DTA curve for (a) MnHCCo; (b) FeHCCo; (c) NiHCCo; (d) ZnHCCo.

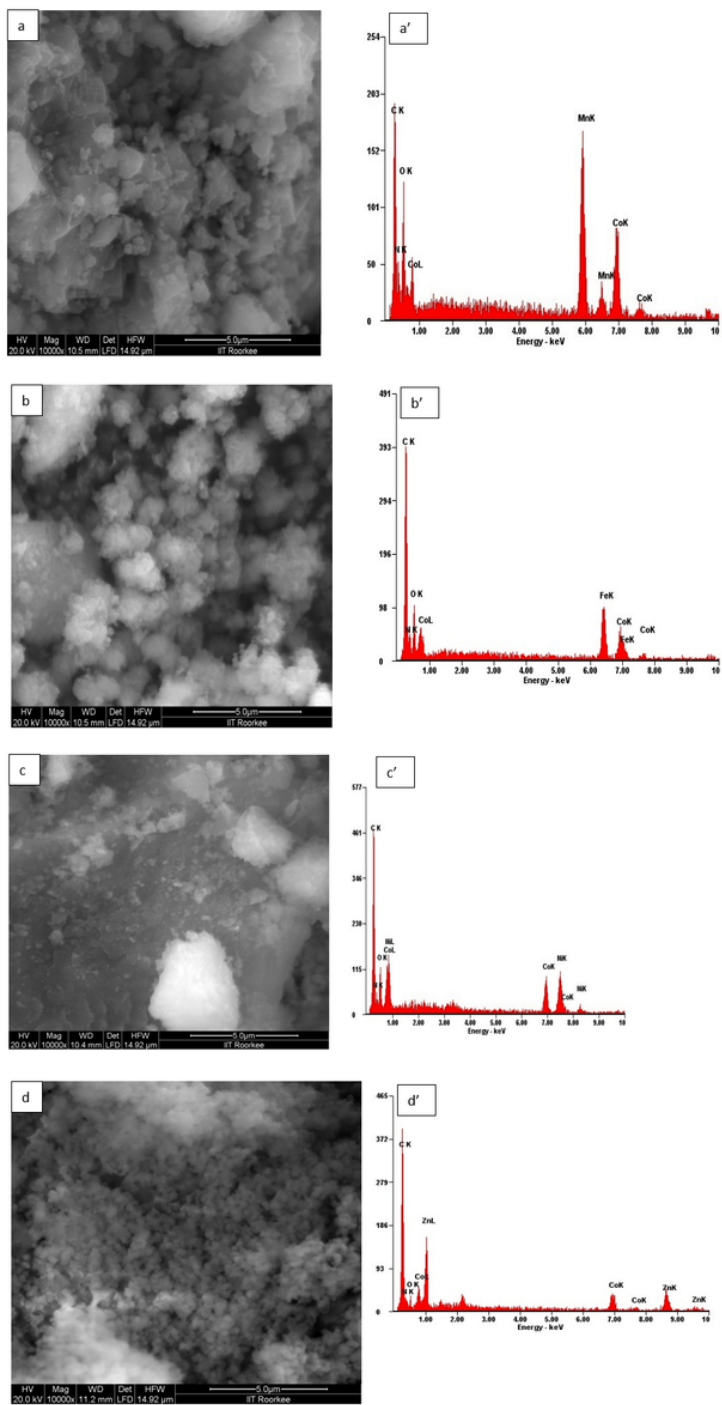


Figure 3

FE-SEM Images and EDX Spectra of (a) MnHCCo; (b) FeHCCo; (c) NiHCCo; (d) ZnHCCo.

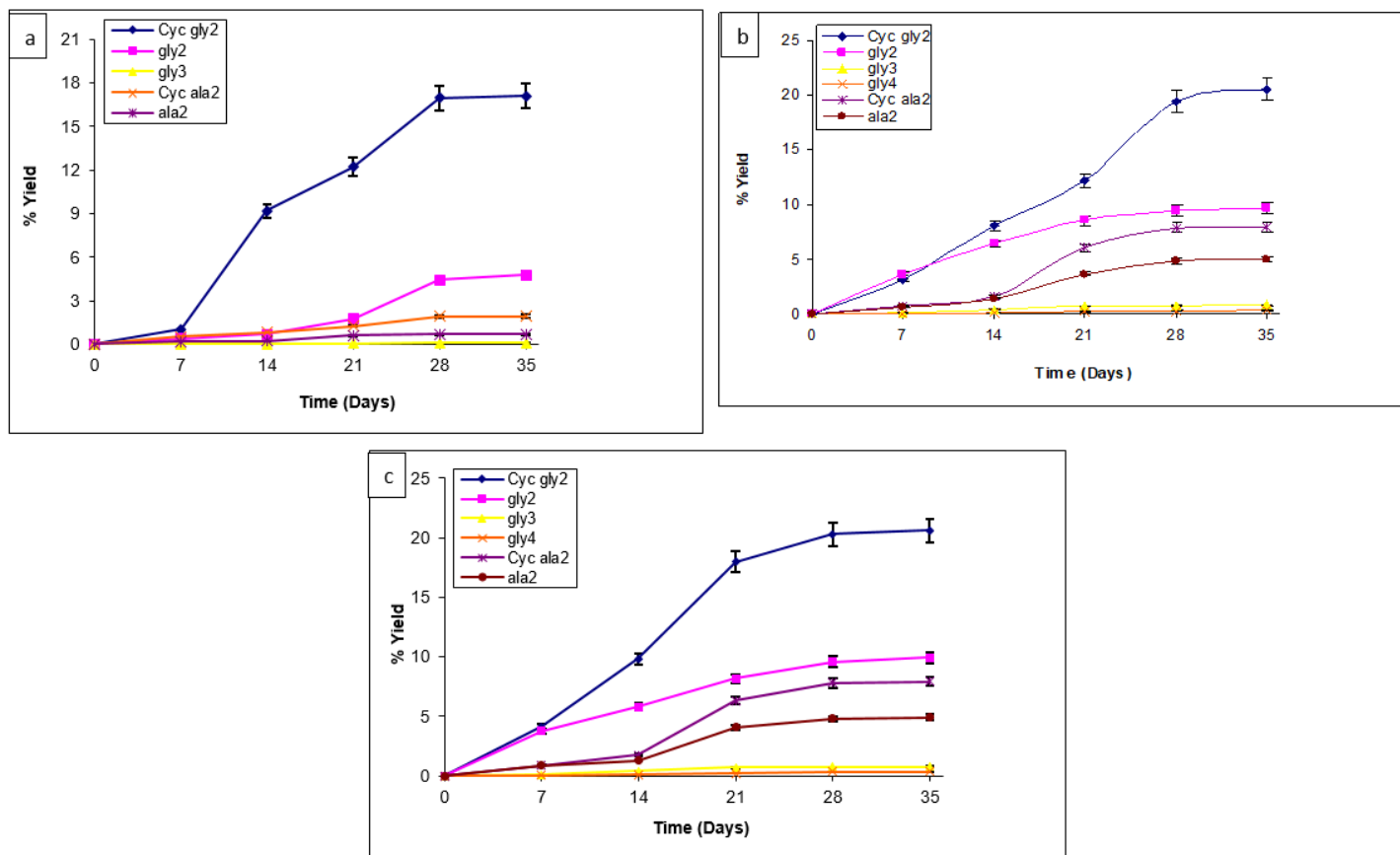


Figure 4

Polymerization of amino acid on MnHCCo complexes at [a] 60, [b] 90, [c] 120°C.

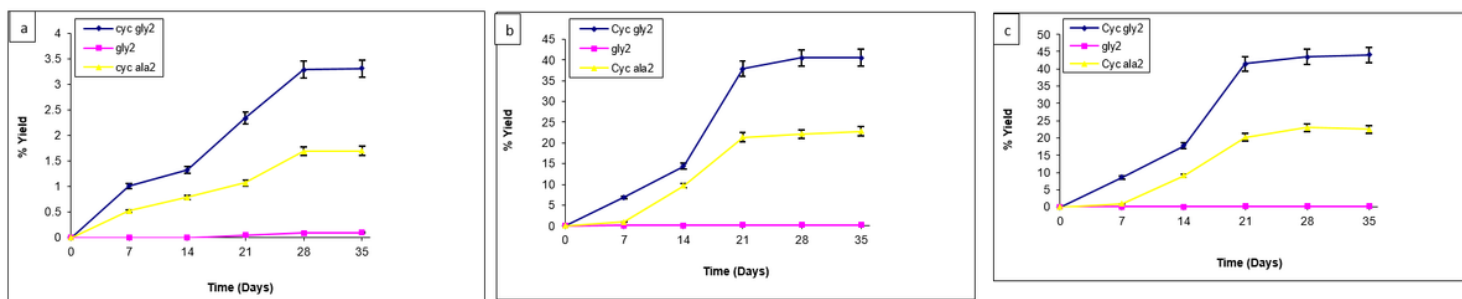


Figure 5

Polymerization of amino acid on FeHCCo complexes at [a] 60, [b] 90, [c] 120°C

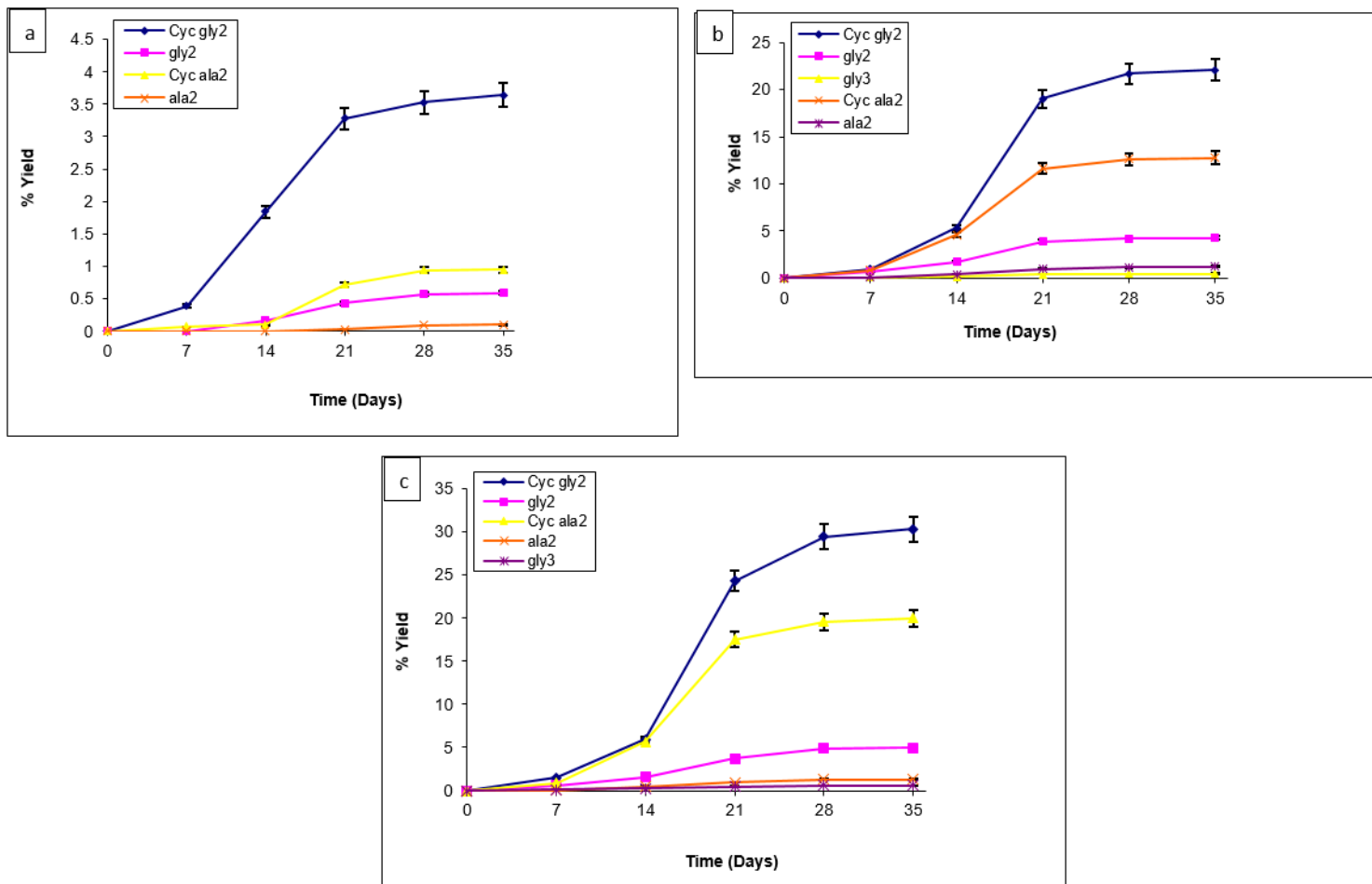


Figure 6

Polymerization of amino acid on NiHCCo complexes at [a] 60, [b] 90, [c] 120°C

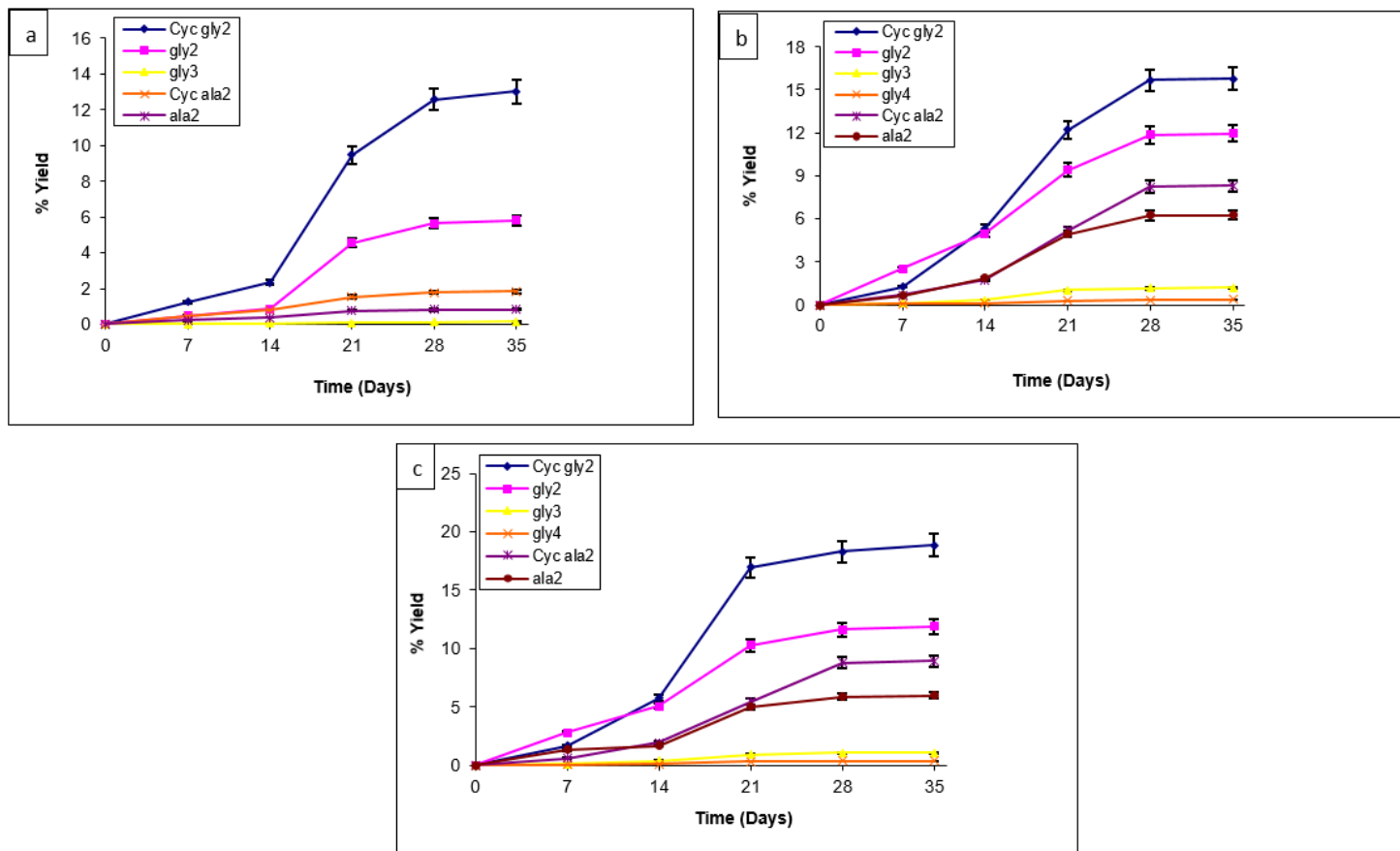


Figure 7

Polymerization of amino acid on ZnHCCo complexes at [a] 60, [b] 90, [c] 120°C

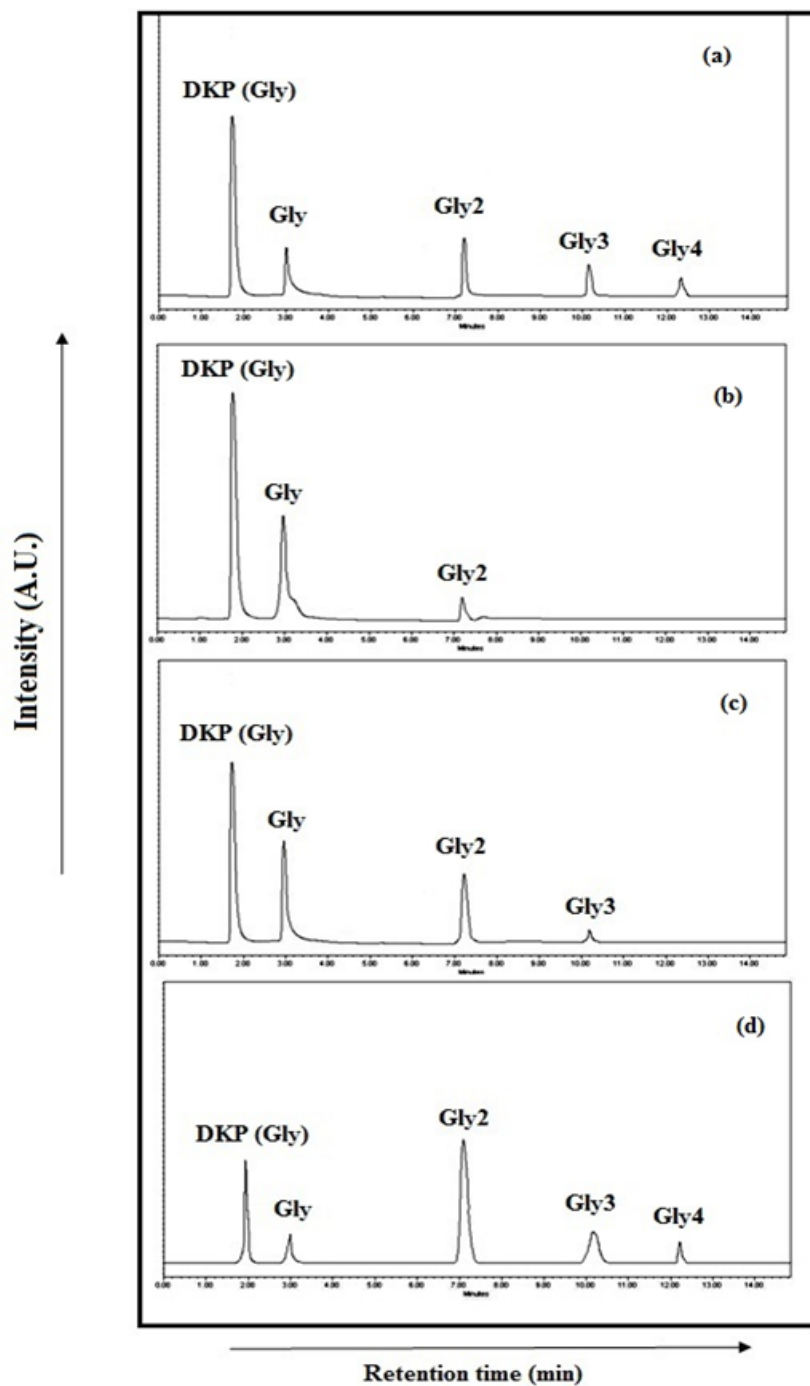


Figure 8

HPLC chromatogram showing the products formed on the surface of [a] MnHCCo,

[b] FeHCCo, [c] NiHCCo, [d] ZnHCCo when glycine was heated at 90 °C on the completion of 4th week.

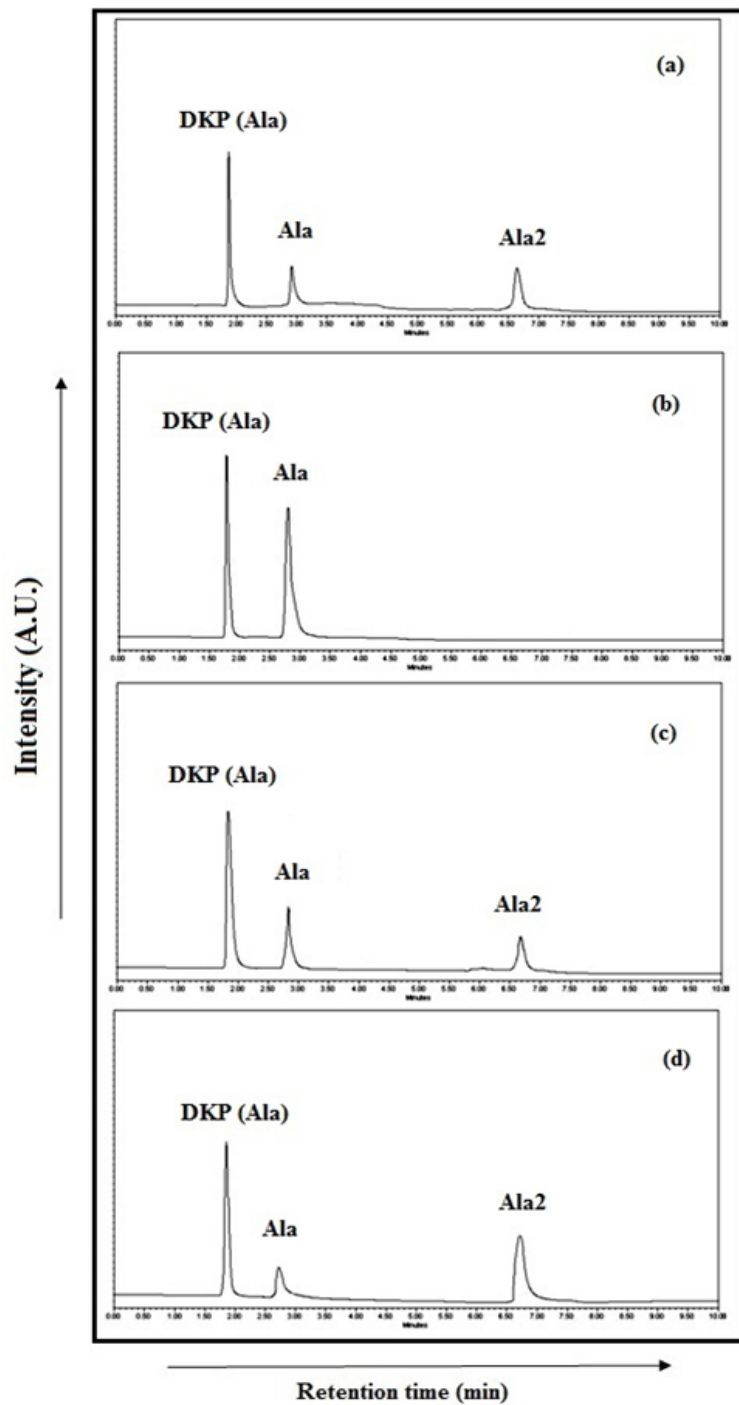


Figure 9

HPLC chromatogram showing the products formed on the surface of [a] MnHCCo,

[b] FeHCCo, [c] NiHCCo, [d] ZnHCCo when alanine was heated at 90 °C on the completion of 4th week.

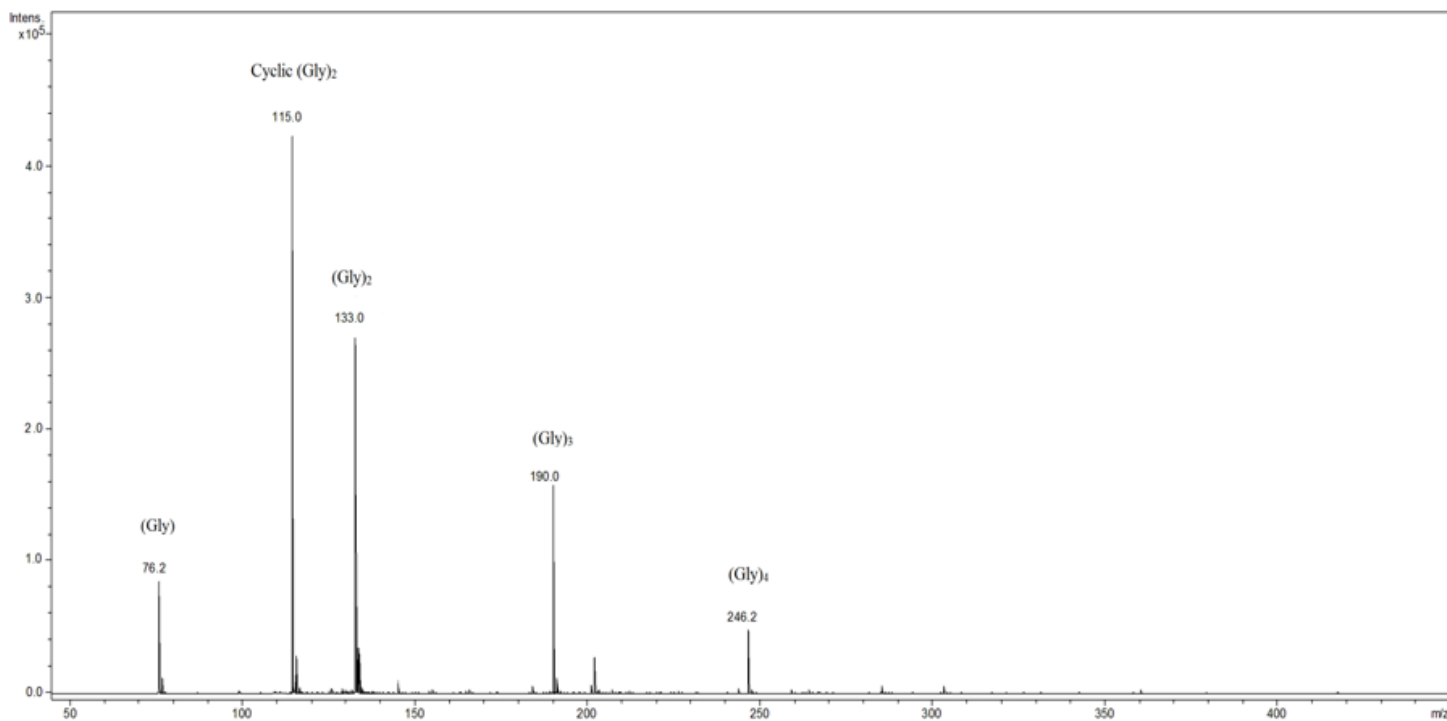


Figure 10

ESI MS spectra of obtained products on surface of ZnHCCo complexes when glycine was heated at 90 °C on the completion of 4th week.

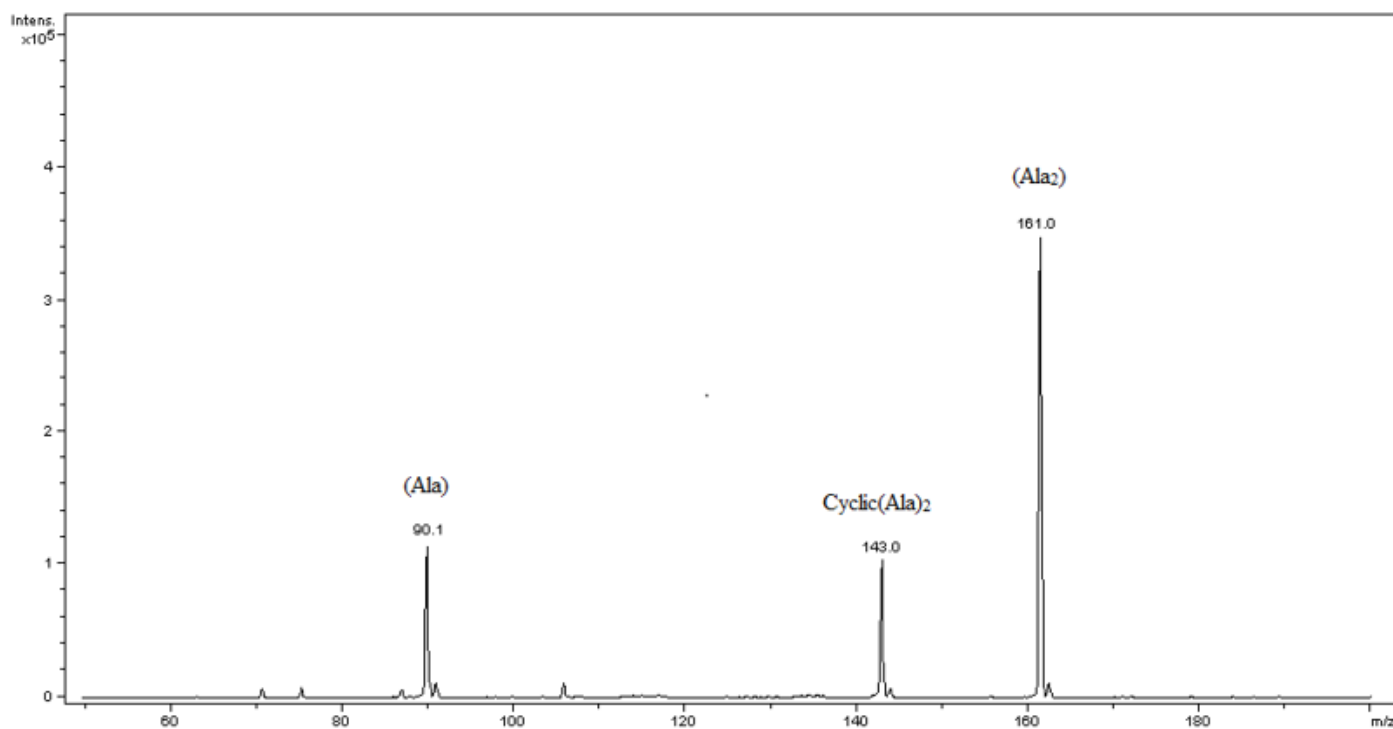


Figure 11

ESI MS spectra of obtained products on surface of ZnHCCo complexes when alanine was heated at 90 °C on the completion of 4th weeks.

Supplementary Files

This is a list of supplementary files associated with this preprint. Click to download.

- [SupportingData.doc](#)